Sub-15 nm Hard X-Ray Focusing with a New Total-Reflection Zone Plate

Hidekazu Takano, Takuya Tsuji*, Takuto Hashimoto, Takahisa Koyama*, Yoshiyuki Tsusaka, and Yasushi Kagoshima

Graduate School of Material Science, University of Hyogo, Kamigori, Hyogo 678-1297, Japan

Received April 30, 2010; accepted June 1, 2010; published online June 18, 2010

A new total-reflection zone plate that consists of a reflective zone pattern with varied-space on a flat substrate was fabricated for hard X-ray nanofocusing. This device is much easier to fabricate than other focusing devices. This is because its focusing size is much smaller than its finest constituent structure since it exploits the effect of glancing X-rays by having a small total reflection angle. Its focusing properties were evaluated using 10-keV X-rays and a focusing size of 14.4 nm was achieved. © 2010 The Japan Society of Applied Physics

DOI: 10.1143/APEX.3.076702

Optical focusing in the hard X-ray region is important since almost all conventional X-ray analytical procedures acquire the high spatial sensitivity using focused X-ray beams. X-ray focusing techniques have developed rapidly due to the development of advanced light sources (especially synchrotron radiation sources) and focusing devices. A focusing device with good focusing properties needs to precisely control X-ray deflection over a wide-angle aperture. Various focusing devices based on diffractive, refractive, and reflective optics have been proposed and developed.[1)] However, some of these conventional devices use a single deflection of the X-ray beam to focus the beam. They employ a single optical element such as a Fresnel zone plate (FZP), a total reflection mirror, or a refractive lens. Consequently, the refractive index of the device defines its fundamental limit for the focusing size, making it difficult to obtain a diffraction-limited size below 10 nm.[2,3)] New devices that can overcome such limits have recently been proposed and developed. A Laue lens configuration based on diffractive optics has been proposed and devices with an approximate structure using varied-thickness multilayers have been developed.[4–6)] In reflective optics, multilayer coatings have been used for reflecting surfaces; a remarkable result of X-ray focusing down to 7 nm has been reported using such optics.[7)] Although these devices have the potential to achieve nanofocusing of hard X-rays, they typically require extremely high-precision fabrication techniques, even for approximate configurations.

Total reflection is an intrinsic phenomenon of hard X-rays. When a pattern on a flat surface reflects an incident X-ray beam, the beam is reflected at a glancing angle. A smaller pattern than the original pattern can then be observed. The reduction ratio is lower than 1/100 because of the small critical angle of total reflection for hard X-rays. This glancing effect can be exploited to form small secondary sources and small apertures based on simple optics. Such devices have been used for Gabor holography,[8)] as a Young's interferometer,[9,10)] and for evaluating focusing.[11)] This effect can also be used to focus hard X-rays. In diffractive optics, the diffraction-limited focusing size is defined by the effective width of the narrowest diffraction zone, so that a zone structure with the size of the desired focusing size needs to be fabricated for a normal-incidence FZP or a Laue lens. By using a pattern of diffraction zones drawn on a flat surface under glancing conditions (see Fig. 1), the effective size of the diffraction zones can be significantly reduced by exploiting the glancing effect. The

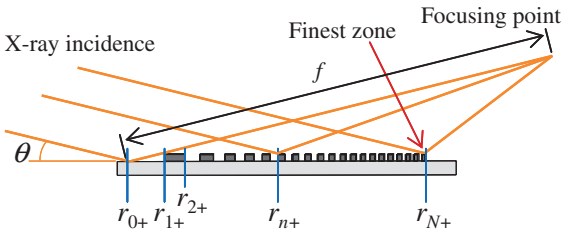

Fig. 1. Schematic drawing of X-ray focusing with a TRZP.

arrangement of the diffraction zones is the same as that for a varied-spacing plane grating,[12)] namely, the optical path difference between adjacent zones is equal to half the wavelength at the focal point. The reflected X-rays at each zone diverge due to diffraction and form a focus by interference. The nth boundary position of each zone r_n is given by

$$r_{n\pm} = \frac{-n\lambda\cos\theta \pm \sqrt{n^2\lambda^2 + 4nf\lambda\sin^2\theta}}{2\sin^2\theta}, \qquad (1)$$

where f is the focal length, θ is the grazing incident angle, and λ is the X-ray wavelength. The zone pattern consists of asymmetric zones of r_{n+} and r_{n-} due to the sign of the second term in eq. (1). This type of focusing device was first proposed by Basov *et al.*, who experimentally performed hard X-ray focusing using a laboratory source.[13)] We have also developed a focusing device, which we term the total reflection zone plate (TRZP), and we used it to obtain a focused beam with a submicron diffraction-limited size using a synchrotron radiation source.[14)] The TRZP is capable of nanofocusing because the focusing size is defined by the small effective zone size. It is difficult to achieve hard X-ray nanofocusing using conventional zone plate optics since X-ray propagation through a structure consisting of very narrow and very thick zones is inhibited by an effect based on dynamical diffraction theory. A great advantage of this device is its ease of fabrication. It is very simple to produce reflective zones on a flat substrate. In addition, this device has much less rigid size and aspect ratios for the zone pattern than for an FZP or a Laue lens.

Table I shows the parameters of the TRZP designed and fabricated in this studied. The designed number of zones N is 1000, the grazing incident angle θ is 6 mrad, the focal length f is 4.16 mm, and the X-ray energy is 10 keV. Based on eq. (1), only half of the full zone that consists of r_{N+} is drawn to prevent the focused beam from overlapping with a direct reflection from the substrate or the minus first-order

*Present affiliation: JASRI/SPring-8.

Table I. Parameters of the fabricated TRZP.

Material of pattern	Pt/Ti (binder)
Thickness of pattern (nm)	10/5 (Pt/Ti)
Number of zones N	1000
X-ray energy (keV)	10
Grazing incident angle θ (mrad)	6
Focal length f (mm)	4.16
Length of zones r_{N+} (mm)	2.44
Finest zone width Δr_{N+} (μm)	0.71
Effective aperture size $r_{N+}\theta$ (μm)	14.6
Diffraction limit by Rayleigh's criterion (nm)	14.6

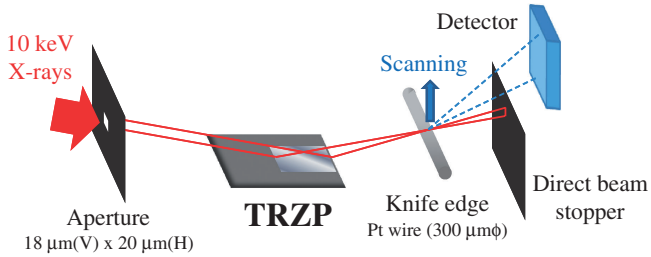

Fig. 2. Experimental set-up for a focusing measurement of the TRZP.

diffraction of the zone pattern. A pattern of zones with a finest dimension of 0.71 μm and the total length of 2.44 mm was drawn using conventional lithographic techniques on a flat silicon wafer as a substrate. A 10-nm-thick platinum layer was used for the zones on a 5-nm-thick titanium binding layer. The intensity of reflection from the substrate is small because the incident angle θ is larger than a critical angle of the substrate. The numerical aperture NA is then given by

$$NA \cong \frac{r_{N+}\theta}{2(f - r_{N+})}. \quad (2)$$

The diffraction-limited focusing size is estimated to be 14.6 nm using Rayleigh's criterion for a rectangular aperture ($0.5\lambda/NA$).

The focusing properties of the TRZP were evaluated using the 24XU "Hyogo-ID" synchrotron radiation beamline of SPring-8.[15] X-rays were monochromatized to 10 keV by a silicon double-crystal monochromator, which has a sufficiently high temporal coherence for the TRZP, and a figure-8 type undulator source provides spatially coherent illumination to the TRZP with an effective aperture size of 14.6 μm. Figure 2 shows a schematic of the measurement configuration used. The intensity distribution of the focusing beam was measured by a knife-edge scanning procedure with a dark-field geometry. This procedure can precisely evaluate the size and shape of a focused beam.[6,16] A 300-μm-diameter platinum wire was used as the knife edge. The angle between the knife edge and the TRZP surface was carefully aligned since the TRZP is a linear focusing device. The knife edge was scanned across the linear focus using a piezoelectric translation stage by closed-loop operation. The TRZP and the knife edge were mounted on a vibration-isolated base that uses air suspension and oil dampers.

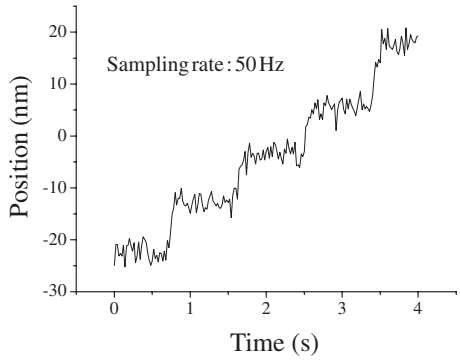

Fig. 3. Translation response of the piezoelectric stage by closed-loop operation.

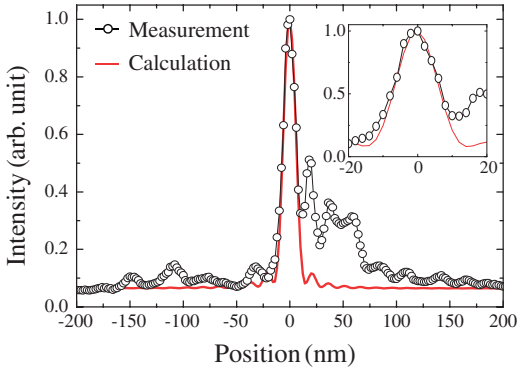

Fig. 4. Intensity distribution of measured (plotted data) and calculated (red line) linear focusing by the TRZP. The inset shows an enlargement of the main peak.

Figure 3 shows the response of the translation stage evaluated by driving it in 10-nm steps. The position stability at each terrace region was evaluated to be 1.6 nm (rms). This response verifies the high motion accuracy of the translation stage. To verify the reliability of the focusing size, measurement with a scan step of 2 nm in the focal plane was repeated 41 times. An average focusing size of 14.4 nm (FWHM) was obtained with a deviation of 1.7 nm (rms). Figure 4 shows a typical profile of the measured intensity. Although the focused beam has some undesirable subpeaks around the main peak, the size of the main peak is close to that estimated by Rayleigh's criterion (14.6 nm). The red line in Fig. 4 indicates the result of numerical calculations based on ray tracing for the TRZP using Fresnel–Kirchhoff integration; it has a FWHM of 13.3 nm.

To investigate the subpeaks in the focused beam, differences between the drawn zones and the designed zones were evaluated. The finest zone width drawn on the substrate could be resolved by an optical microscope, so that the differences can be measured directly from the distance between adjacent zone boundaries. Although the total length of zones drawn is smaller (2.43 mm) than the designed value (2.44 mm), the zone arrangement could be fitted using eq. (1) by varying the focal length (4.14 mm) and the grazing incident angle (6.01 mrad). Figure 5 shows the optical path difference for each zone number n, which was obtained from the difference between the measured value

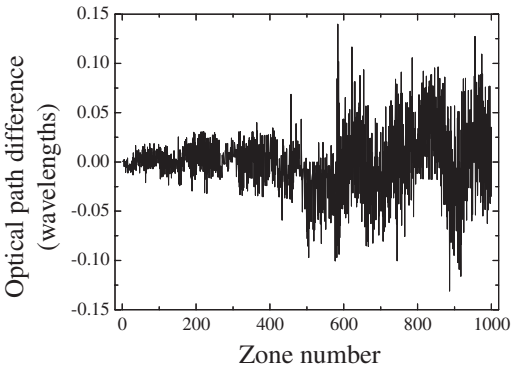

Fig. 5. Optical path difference between a drawn pattern and an ideal pattern fitted with a focal length of 4.14 mm and a grazing incident angle of 6.01 mrad at every zone of the TRZP.

and the fitted curve. The results reveal that no significant aberrations are caused by pattern-drawing errors since all the drawn zones satisfy the condition that the deviation of the optical path difference be less than a quarter of a wavelength. Therefore, unevenness in the substrate is considered to cause aberrations, such as subpeaks. A conventional 0.5-mm-thick silicon wafer was used as the substrate for the fabricated TRZP, and warping due to stress as a result of zone deposition may occur. The substrate of a TRZP needs to have a flatness of a few nanometers to achieve its ultimate focusing capability; this is not difficult, since such substrates are commercially available (e.g., X-ray plane mirrors for energy cut-off). In the TRZP, the finest effective zone size $\Delta r_{N+\_\mathrm{eff}}$ is approximately given by

$$\Delta r_{N+\_\mathrm{eff}} \cong \frac{\Delta r_{N+}\theta}{(1 - r_{N+}/f)}. \quad (3)$$

This shows that the glancing effect of the TRZP becomes small when the focal size of TRZP is small (i.e., r_{N+}/f is close to unity). This makes it harder to fabricate a TRZP, and may provide a practical limit for the focusing size of a TRZP. The surface roughness of the reflective pattern also influences the practical limit. However, the device developed in this study has the potential to achieve a focusing size of 5 nm or better in the near future.

1) A. Snigirev and I. Snigireva: C. R. Physique **9** (2008) 507.
2) C. Bergemann, H. Keymeulen, and J. F. van der Veen: Phys. Rev. Lett. **91** (2003) 204801.
3) Y. Suzuki: Jpn. J. Appl. Phys. **43** (2004) 7311.
4) H. C. Kang, H. Yan, R. P. Winarski, M. V. Holt, J. Maser, C. Liu, R. Conley, S. Vogt, A. T. Macrander, and G. B. Stephenson: Appl. Phys. Lett. **92** (2008) 221114.
5) H. Yan, H. C. Kang, J. Maser, and G. B. Stephenson: Rev. Sci. Instrum. **79** (2008) 053104.
6) T. Koyama, S. Ichimaru, T. Tsuji, H. Takano, Y. Kagoshima, T. Ohchi, and H. Takenaka: Appl. Phys. Express **1** (2008) 117003.
7) H. Mimura, S. Handa, T. Kimura, H. Yumoto, D. Yamakawa, H. Yokoyama, S. Matsuyama, K. Inagaki, K. Yamamura, Y. Sano, K. Tamasaku, Y. Nishino, M. Yabashi, T. Ishikawa, and K. Yamauchi: Nat. Phys. **6** (2010) 122.
8) S. Aoki, N. Watanabe, T. Ohigashi, H. Yokosuka, Y. Suzuki, A. Takeuchi, and H. Takano: Jpn. J. Appl. Phys. **44** (2005) 417.
9) W. Leitenberger and U. Pietsch: J. Synchrotron Rad. **14** (2007) 196.
10) T. Tsuji, T. Koyama, H. Takano, Y. Tsusaka, and Y. Kagoshima: J. Phys.: Conf. Ser. **186** (2009) 012061.
11) O. Hignette, G. Rostaing, P. Cloetens, A. Rommeveaux, W. Ludwing, and A. Freund: Proc. SPIE **4499** (2001) 105.
12) M. Itou, T. Harada, and T. Kita: Appl. Opt. **28** (1989) 146.
13) Y. A. Basov, D. V. Roshchupkin, I. A. Schelokov, and A. E. Yakshin: Proc. 4th Int. Conf. X-ray Microscopy, 1993, p. 593.
14) T. Tsuji, H. Takano, T. Koyama, Y. Tsusaka, and Y. Kagoshima: Jpn. J. Appl. Phys. **49** (2010) 030207.
15) Y. Tsusaka, K. Yokoyama, S. Takeda, K. Takai, Y. Kagoshima, and J. Matsui: Nucl. Instrum. Methods A **467–468** (2001) 670.
16) Y. Suzuki, A. Takeuchi, H. Takano, and H. Takenaka: Jpn. J. Appl. Phys. **44** (2005) 1994.